INTERNATIONAL JOURNAL FOR NUMERICAL METHODS IN FLUIDS, VOL. 21, 113–127 (1995)

CALCULATION OF COMPLEX NEAR-WALL TURBULENT FLOWS WITH A LOW-REYNOLDS-NUMBER k–ε MODEL

P. KOUTMOS AND N. C. KOSTOUROS

Department of Mechanical Engineering, University of Patras, Patras, Rio 26110, Greece

SUMMARY

An improved low-Reynolds-number k–ε model has been formulated and tested against a range of DNS (direct numerical simulation) and experimental data for channel and complex shear layer flows. The model utilizes a new form of damping function adopted to account for both wall proximity effects and viscosity influences and a more flexible damping argument based on the gradient of the turbulent kinetic energy on the wall. Additionally, the extra production of the inhomogeneous part of the viscous dissipation near a wall has been added to the dissipation equation with significantly improved results. The proposed model was successfully applied to the calculation of a range of wall shear layers in zero, adverse and favourable pressure gradients as well as backward-facing-step separated flows.

KEY WORDS turbulence modelling; k–ε model; wall damping; channel flow; boundary layer flow

1. INTRODUCTION

A large number of important engineering and scientific calculations of turbulent flows have been based on one-point, two-equation eddy viscosity turbulence models. For high-Reynolds-number flows the k–ε model of Launder and Spalding[1] is the most widely used, representing a compromise between zero- or one-equation and second-order closures.[2] For calculations involving flows adjacent to solid boundaries the standard version of the model has been used in conjunction with wall functions.[1] This approach, however, is unsatisfactory[3] for calculations of complex near-wall flows, when assumptions of a logarithmic velocity profile, local equilibrium and uniform shear stress behaviour are not valid.[4] With increases in computer power the aforementioned drawbacks may be partly overcome if the integration of the transport equations is carried all the way to the wall.[5] The effort is then directed towards extending the standard model to account for the limiting behaviour of the near-wall turbulent processes.[6,7]

The various low-Reynolds-number k–ε model versions developed so far have been appraised and evaluated by Patel *et al.*,[8] Lang and Shih[9] and Michelassi and Shih.[10] The key element in the success of these models is the consistent use of turbulent-Reynolds-number-dependent damping functions and extra terms produced by dimensional reasoning, data fitting and indirect testing with the aim of reproducing the observed near-wall behaviour.

A computationally more economical approach is to use two-layer models.[11] There the length scale variation near a wall is exploited for the algebraic description of the dissipation while solving only for the better-formulated k equation. The method needs further testing, but the prescription of a near-wall length scale distribution (implying neglect of turbulent transport) and the resulting algebraic expression for the dissipation may be a dubious practice when sudden changes occur in the near-wall turbulent structure.[3,12]

CCC 0271–2091/95/020113–15

Received March 1994
Revised October 1994

Another approach that has recently emerged as a novel methodology for consistently prescribing corrections to the k–ε equations is the method of renormalization group theory.[13] Although this approach shows promise in obtaining terms that account for non-equilibrium effects[14] (e.g. extra strain rates, rotation, wall effects), it requires further testing and verification before it is considered for wider application.[15]

In recent years, direct numerical simulation (DNS) databases[12,16–18] have allowed a better understanding of near-wall turbulence while enabling a direct and more accurate testing of low-Reynolds-number turbulence models. DNS data have been used by several authors as an aid in constructing new model components and testing and improving their performance.[7,19–21]

Despite rapid developments, however, deficiencies still exist in current versions of low-Reynolds-number k–ε models.[9,10] Some are addressed in this work. The damping of turbulent transfer near a wall is caused (partly) by the influence of viscosity and (mainly) by the 'flattening' of the turbulent structure due to wall proximity.[8,22] This is solely accounted for by curve fitting of DNS solutions, an approach that has frequently been questioned. Here it is proposed to include both the above effects via the use of a variable parameter c_μ obtained from reduction of algebraic stress relationships. In addition, the argument used in the damping function is often based on the friction velocity or the turbulent kinetic energy, which varies with normal distance. In this study an equivalent RMS friction velocity defined on the wall is chosen instead on the basis of experimental evidence[23] and the benefits of this are discussed below.

A further aspect of the present work is the effort to improve the near-wall modelling of the dissipation equation. Firstly, the introduction of a pseudo dissipation is here obviated through the use of a multiple-time-scale model[21] which is now extended to account for the time scale transition in the buffer layer. Secondly, the difficulty in reproducing the 'exact' ε DNS profile near the wall is addressed. A number of extra terms have been attempted,[19,20] but a simple and numerically robust ε equation that contributes to the correct prediction of ε near the wall within the context of the eddy viscosity approach has yet to emerge. In the present study the extra production of the inhomogeneous part of the viscous dissipation is simply added to the proposed ε equation with significant benefit.

The present contribution describes a number of suggestions which improve over existing models on all the previously discussed issues. This is achieved without further increases in complexity whilst the presented model retains its high-Reynolds-number form away from solid boundaries. Details of the model improvements are discussed in the following section. The predictive performance of the model is assessed by calculating fully developed channel flows and boundary layers in zero, adverse and favourable pressure gradients as well as separated flows and comparing the computational results with available DNS and experimental data.

2. PROPOSED MODEL

The continuity and Reynolds-averaged Navier–Stokes equations describing incompressible turbulent flow can be written as

$$U_{i,i} = 0, \tag{1}$$

$$\dot{U}_i + U_j U_{i,j} = -\frac{1}{\rho} P_{,i} + \nu U_{i,jj} - \overline{(u_i u_j)}_{,j}, \tag{2}$$

where U and P are the mean velocity and pressure respectively and an index, i denotes the partial derivative with respect to x_i.

Within the eddy viscosity concept the Reynolds stresses $\overline{u_i u_j}$ are related to the mean field as

$$-\overline{u_i u_j} = \nu_t(U_{i,j} + U_{j,i}) - \tfrac{2}{3}k\delta_{i,j}, \tag{3}$$

where ν_t is the eddy viscosity and k is the kinetic energy of turbulence. The scalar eddy viscosity is determined from a turbulent velocity scale $u_t \sim k^{1/2}$ and a turbulent length scale $l_t = k^{3/2}/\varepsilon$, where ε is the dissipation rate of turbulent kinetic energy. The eddy viscosity is then given by

$$\nu_t = c_\mu f_\mu \frac{k^2}{\varepsilon}, \tag{4}$$

where c_μ is usually taken as constant and f_μ is a damping function. k and ε may be obtained from the modelled transport equations[1,4]

$$\dot{k} + U_j k_{,j} = \left[\left(\nu + \frac{\nu_t}{\sigma_k}\right)k_{,j}\right]_{,j} + P_k - \varepsilon, \tag{5}$$

$$\dot{\varepsilon} + U_j \varepsilon_{,j} = \left[\left(\nu + \frac{\nu_t}{\sigma_\varepsilon}\right)\varepsilon_{,j}\right]_{,j} + c_{\varepsilon 1} f_1 \frac{P_k}{\tau} - C_{\varepsilon 2} f_2 \frac{\varepsilon}{\tau} + E, \tag{6}$$

where $\tau = k/\varepsilon$ is the turbulent time scale. The damping functions f_μ, f_1, f_2 and the extra term(s) E are usually employed to account for low-Reynolds-number effects when the above equations are integrated up to the solid boundary.[4]

In the above form with $f_\mu = 1$, $f_1 = f_2 = 1, E = 0$ and the constants $c_{\mu_0} = 0{\cdot}09$, $c_{\varepsilon 1} = 1{\cdot}44$, $c_{\varepsilon 2} = 1{\cdot}92$, $\sigma_k = 1{\cdot}0$ and $\sigma_\varepsilon = 1{\cdot}3$, equations (4)–(6) comprise the standard high-Reynolds-number version of the k–ε model.[1]

Customarily the influences of wall proximity and molecular viscosity upon turbulent momentum transfer have been introduced into the model in a common fashion, i.e. through the use of the damping function f_μ.[3] It is recognized[4,24] that the reduction of the turbulent viscosity near a solid boundary is influenced much more by the suppression of normal velocity fluctuations due to wall presence than by the effect of viscous action. It should also be noted that the former mechanism is related to the Reynolds stress redistribution process via the pressure strain rate term. An additional and equally important aspect of the limiting behaviour of near-wall turbulent transprot is that high shear rate alone can produce a significant enhancement of the streamwise velocity fluctuations at the expense of the normal components, as suggested by Lee *et al.*[22] All the above-mentioned effects should be accounted for within a model formulation to make it widely applicable.

Currently popular damping functions produced by curve fitting of DNS or experimental results for simple flows cannot be expected to capture variations in turbulent structure as they occur in more complex flows.[24]

Here it is suggested that the first and third of the above-discussed effects be included via a variable coefficient c_μ. Indeed, a constant value c_μ has long been in question, while recent DNS results[25] have indicated that the product $c_\mu f_\mu$ is a function of the ratio P_k/ε. A number of expressions for a variable c_μ have been obtained for thin shear layers by reduction of algebraic stress models.[2] One of the simplest[2] has been chosen for initial study, i.e.

$$c_\mu = 1{\cdot}5\frac{(1 - c_2)(c_1 - 1 + c_2 P_k/\varepsilon)}{(c_1 - 1 + P_k/\varepsilon)^2}. \tag{7}$$

Since the ratio P_k/ε can be reformulated as $P_k/\varepsilon = c_\mu f_\mu S^2$, where $S = (k/\varepsilon)\,\partial U/\partial y$ is the shear rate parameter discussed in Reference 22, the above form also embodies the influence of the shear rate. The variation in $c_\mu(P_k/\varepsilon)$ for fully developed channel flow with P_k and ε obtained from DNS data is

depicted in Figure 1(a). The inherent damping nature of this expression is clearly illustrated, supporting its employment in the damping product $c_\mu f_\mu$. However, if one plots the 'exact' expression $c_y = -\overline{uv}(\varepsilon/k^2)(\partial u/\partial y)^{-1}$ (see Figure 1(a)) evaluated from DNS data, it is apparent that equation (7) alone is insufficient to reproduce the correct damping. The discrepancy is believed to stem mainly from the omissison of the wall reflection terms in the pressure strain model used for the derivation of the c_μ function.[2] Suitable inclusion of these effects might eliminate the difference and hence the need for any further form of damping. This of course would also entail increased complexity in the form of a Reynolds stress closure for the viscous sublayer, which is currently under rigorous development. Some of the important effects discussed above are already included through the c_μ expression and at this level of closure near-wall damping is simply supplemented by multipying the expression $c_\mu(P_k/\varepsilon)$ by a function of the form

$$f_\mu = 0{\cdot}5c_{\mu 0} + (1 - 0{\cdot}5c_{\mu 0})\left[1 - \exp\left(-\frac{y^* - y_v^*}{A^*}\right)\right]^2, \tag{8}$$

with $c_{\mu 0} = 0{\cdot}09$. This varies asymptotically as y^{-1} near the wall, as discussed in Reference 25. It has also been argued that the frequently used f_μ argument $y^+ = yu_\tau/\nu$ is generally unsuited for separated flows.[4] For such flows, experimental data[23] suggest that the near-wall turbulent kinetic energy is better correlated by the RMS of the friction velocity rather than the friction velocity itself. Therefore the

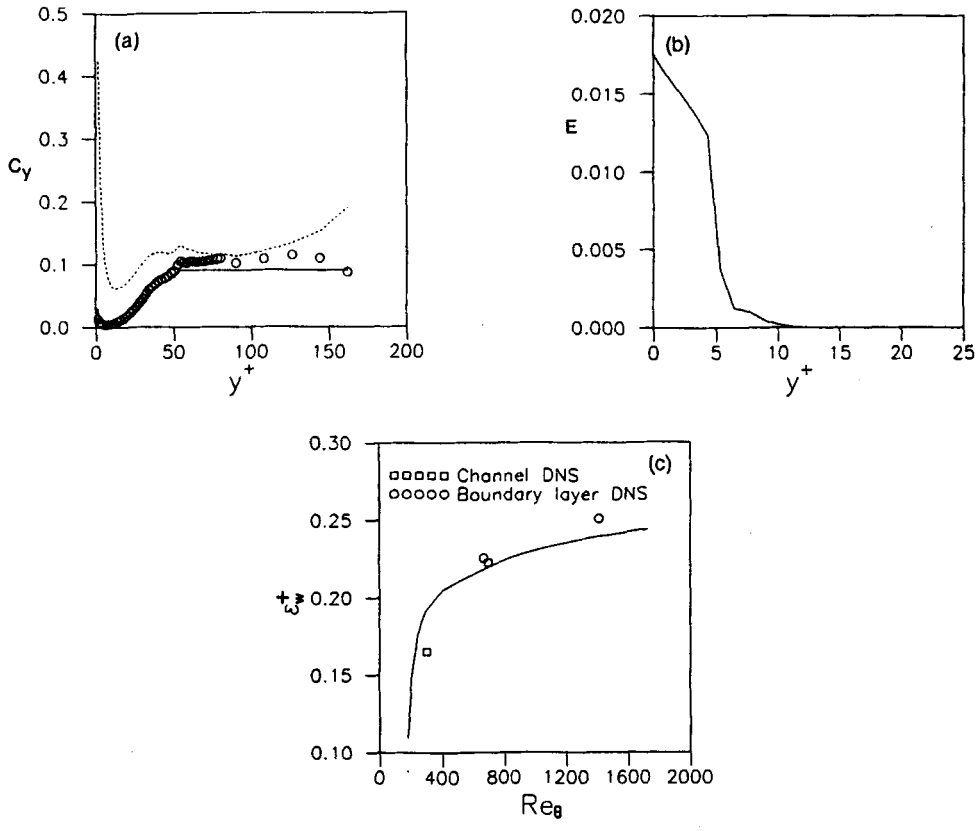

Figure 1. (a) Proposed damping function c_y compared with DNS data:\; – – –, $c_\mu(P_k/\varepsilon)$; ——, c_y; o, DNS. (b) Near-wall distribution of the proposed extra term E in the dissipation equation. (c) Asymptotic variation in the wall dissipation: ○, DNS; ————, present predictions

argument used here is taken as

$$y^* = \frac{yu_\tau^*}{\nu}, \tag{9}$$

where u_τ^* is an equivalent RMS friction velocity defined as

$$u_\tau^* = \nu\left(\frac{\partial k^{1/2}}{\partial y}\right)^{1/2}. \tag{10}$$

Reformulation of (10) suggests that

$$u_\tau^* = \left(\frac{\nu\varepsilon_w}{2}\right)^{1/4} \tag{11}$$

and for $u_\tau \neq 0$ we observe that the ratio u_τ^*/u_τ is

$$\lambda = \frac{u_\tau^*}{u_\tau} = \left(\frac{\varepsilon_w^+}{2}\right)^{1/4}, \tag{12}$$

where ε_w is the wall dissipation given as

$$\varepsilon_w = 2\nu\left(\frac{\partial k^{1/2}}{\partial y}\right)_w^2, \qquad \varepsilon_w^+ = \frac{\varepsilon_w \nu}{u_\tau^4}. \tag{13}$$

In equation (8) we take $y_v^* = \lambda y_v^+$, where $y_v^+ = 4$ (the viscous sublayer thickness for equilibrium layers), and $A^* = 15$.

The constants in expression (7), where optimized by analytical fitting of DNS data and in the final values were adjsuted (only slightly) during the flow tests. The constants thus obtained are $c_1 = 1{\cdot}2$ and $c_2 = 1{\cdot}9$.

The final form of the damping function used here is therefore

$$c_y = c_\mu(P_k/\varepsilon)f_\mu(y^*) \tag{14}$$

and reproduces the DNS data well, as shown in Figure 1(a). The upper limit value for the damping product is taken as 0·09 so that the model reverts to its high-*Re* version away from the wall.

A further aspect of the proposed model is the employment of a multiple time scale in the ε equation. The use of a variable time scale[21] utilizes the Kolmogorov behaviour of near-wall turbulence (where $\tau_k = \sqrt{\nu/\varepsilon}$), whilst the large-eddy time scale ($\tau_\tau = k/\varepsilon$) pertains away from the wall. The above concept is here extended to include the time scale transition occurring in the buffer region, as follows:

$$\tau = \begin{cases} c_k\tau_k, & \tau_t < c_k\tau_k, \\ 0{\cdot}5(c_k\tau_k + c_B\tau_k), & c_k\tau_k < \tau_t < c_B\tau_k, \\ \tau_t, & \tau_t > c_B\tau_k, \end{cases} \tag{15}$$

where the constants c_k and c_B take values of 3·74 and 15·7 which correspond to the values of the ratio τ_t/τ_k at the edge of the viscous sublayer ($y^+ = 4$) and the buffer region ($y^+ = 30$) respectively according to DNS data.[16–18]

Within the context of the modelling of the dissipation equation the adequate calculation of the ε profile in the sublayer region[19] is subsequently addressed. The contribution of the inhomogeneous part of the wall dissipation $D = 2\nu(\partial k^{1/2}/\partial y)^2$ to the overall ε profile in the wall region has been accounted for here through an extra term in the ε equation which has the form.

$$E = \left(A + \frac{B}{Re^*}\right)\frac{D}{\sqrt{(\nu/D)}}, \tag{16}$$

where $Re^* = (u_\tau^* \delta / \nu$ (δ is the channel half-width or boundary layer thickness).

With this term the production of the inhomogeneous part of ε near a wall is included through the anisotropic part of the dissipation combined with an appropriate time scale $\sqrt{(\nu/D)}$. The constants A and B take values of 0·22 and 25·22 and were optimized with the aid of DNS data. Figure 1(b) shows the distribution of this term evaluated analytically from DNS data and suggests that its influence is confined to the sublayer region. Figure 1(c) presents the calculated (in the flow tests discussed below) ε_w^+ distribution in a developing boundary layer. Clearly the inclusion of this term helps to reproduce adequately the DNS results.

When dealing with flows where departures from equilibrium occur (due to pressure gradient, heating, suction, etc.), it has been found[26] necessary to restrain the abnormal time scale growth by multiplying the constant $c_{\varepsilon 1}$ in the ε equation by a factor $1 + 0 \cdot 1 c_\nu S^2$, where S is the shear rate parameter. This near-wall correction is applied to the axial station whenever the ratio of the near-wall peak value of the turbulent energy production (usually occurring at around $y^+ = 10$) to the wall dissipation value, i.e. the ratio $P_{k\max}/\varepsilon_w$, is outside the range (0·95, 1·3).

In summary then, the proposed model is

$$\dot{k} + U_j k_{,j} = \left[\left(\nu + \frac{\nu_t}{\sigma_k}\right) k_{,j}\right]_{,j} + P_k - \varepsilon,$$

$$\dot{\varepsilon} + U_j \varepsilon_{,j} = \left[\left(\nu + \frac{\nu_t}{\sigma_\varepsilon}\right) \varepsilon_{,j}\right]_{,j} + c_{\varepsilon 1} \frac{P_k}{\tau} - c_{\varepsilon 2} \frac{\varepsilon}{\tau} + E,$$

$$\nu_t = c_\nu \frac{k^2}{\varepsilon}, \qquad c_\nu = c_\mu (P_k/\varepsilon) f_\mu(y^*),$$

$$c_\mu(P_k/\varepsilon) = 1 \cdot 3 \frac{(1 - c_2)(c_1 - 1 + c_2 P_k/\varepsilon)}{(c_1 - 1 + P_k/\varepsilon)^2},$$

$$f_\mu(y^*) = 0 \cdot 5 c_{\mu 0} + (1 - 0 \cdot 5 c_{\mu 0}) \left[1 - \exp\left(-\frac{y^* - y_v^*}{A^*}\right)\right]^2,$$

$$y^* = \frac{y u_\tau^*}{\nu}, \qquad u_\tau^* = (\nu \sqrt{k_{,y}})_w^{1/2},$$

$$\tau = \begin{cases} c_k \tau_k & \tau_t < c_k \tau_k \\ 0 \cdot 5 (c_k \tau_k + \tau_t), & c_k \tau_k < \tau_t < c_B \tau_k, \\ \tau_t, & \tau_t > c_B \tau_k, \end{cases}$$

with

$$E = \left(A + \frac{B}{Re^*}\right) \frac{D}{\sqrt{(\nu/D)}}, \qquad D = 2\nu(\sqrt{k_{,y}})^2, \qquad Re^* = \frac{u_\tau^* \delta}{\nu},$$

$$c_1 = 1 \cdot 2, \qquad c_2 = 1 \cdot 9, \qquad c_{\mu 0} = 0 \cdot 09, \qquad y_v^* = \lambda y_v^+, \qquad y_v^+ = 4,$$

$$A^* = 15, \qquad c_k = 3 \cdot 74, \qquad c_B = 15 \cdot 7, \qquad A = 0 \cdot 22, \qquad B = 25 \cdot 22.$$

3. COMPUTATIONAL DETAILS

The proposed low-Reynolds-number k–ε model was implemented into a 2D finite volume code for incompressible flow with recirculation employing a staggered mesh and the QUICK differencing scheme for the convection terms. The formulation comprised a linearized implicit pressure correction method (Simpler[27]) and the discretized equations are solved implicitly using a tridiagonal matrix algorithm. Details of the code can be found in Reference 28.

A semi-elliptic calculation was performed for the flows considered here whereby the pressure gradient was imposed on the streamwise momentum equation without solving the pressure equation. This amounts to applying a boundary layer approximation. The longer run times necessary for this type of solution were acceptable, since the intention is to use the model in complex flows. A few test cases were also run with GENMIX type of code and identical results were obtained with the two methods.

Three meshes of 41×31, 100×56 and 150×80 (x,y) grid nodes were used to check grid independence. The two finer meshes produced nearly identical results and the 100×56 mesh was used for all subsequent calculations. The first three grid nodes near the wall were placed at y^+ distances of 0·0583, 0·215 and 0·484 respectively.

All runs were performed on a Hewlett-Packard HP720 Risc System.

The boundary conditions used are

$$U = k = 0 \quad \text{and} \quad \varepsilon_w = 2\nu k/y^2 \quad \text{at } y = 0 \text{ (wall)}$$

and

$$\frac{\partial U}{\partial y} = \frac{\partial k}{\partial y} = \frac{\partial \varepsilon}{\partial y} = 0 \quad \text{at the channel axis (channel flow)}$$

or

$$U = U_\infty \quad \text{and} \quad \varepsilon = k = 0 \quad \text{at the freestream (boundary layer).}$$

For the case of zero-pressure-gradient (ZPG) channel and boundary layer flows, constant values are prescribed as initial profiles for the solved quantities and the solution develops into its similarity form. The sensitivity of the solutions to the inlet k and ε profiles was also examined. For ZPG boundary layer calculations inlet values of k were taken as 1% of u_∞^2 and the ε profile was claculated as const. $\times\, k^{3/2}/c_L y$ (c_L =2·5). When the resulting inlet ratio ν_t/ν was in the range 2–4 there was no effect on the results. Variation of this ratio by 15–20% had an effect on the computations up to $Re_\theta = 1000$. Beyond this Re_θ the results were insensitive to inlet-assigned values. The constant in the above ε expression was therefore utilized to adjust this variation. For pipe flow calculations, roughly similar observations were made: arbitrary inlet profiles would develop into their self-similar form. The run times were, however, significantly reduced when all inlet profiles were taken from DNS solutions at the Reynolds number calculated.

For boundary layers in adverse or favourable pressure gradients, initial conditions are obtained by starting with a zero-pressure-gradient boundary layer and then subjecting it to the experimentally reported pressure gradient districution at an axial position determined by the value of Re_θ found from experiment.

4. RESULTS AND DISCUSSION

The proposed model (termed PR) was tested by calculating the following flows: fully developed channel flows at $Re_\tau = 180$, 395 (the DNS data of References 16–18) and 1052 (the measurements of Laufer[29]); a boundary layer flow developing at zero pressure gradient up to $Re_\theta = 16{,}465$ (the data of

Weighard and Tillman[30] and Klebanoff[31] as well as the DNS data of Spalart[18] at $Re_\theta = 1410$); a boundary layer developing under a strong adverse pressure gradient (APG—the data of Nagano *et al.*[32]); the relaminarizing boundary layer of Patel and Head[33] developing under a strong favourable pressure gradient (FPG); the separating rearward-facing step flow of Driver and Seegmiller.[34]

4.1. ZPG channel and boundary layer flows

Figures 2–4 depict the calculated profiles of (a) mean velocity, (b) turbulent shear stress, (c) kinetic energy and (d) dissipation in wall co-ordinates for channel flow at $Re_\tau = 180$, 395 and 1052 respectively. Predictions obtained with one of the more recent and successful models, that of Michelassi *et al.*[20] (termed RMM), are also included. The RMM model uses a different form of damping and achieved an improved prediction of the ε profile through a different formulation. Careful placement of near-wall grid nodes was, however, necessary with this model owing to numerical instabilities.

The predicted velocity distributions obtained by the two models are indistinguishable for $Re_\tau = 395$ (Figure 3(a)), while the PR model slightly underestimates the velocity near the centreline for $Re_\tau = 180$. This may be traced to the use of the present damping formulation and the function $c_\mu(P_k/\varepsilon)$, but the disagreement is only moderate.

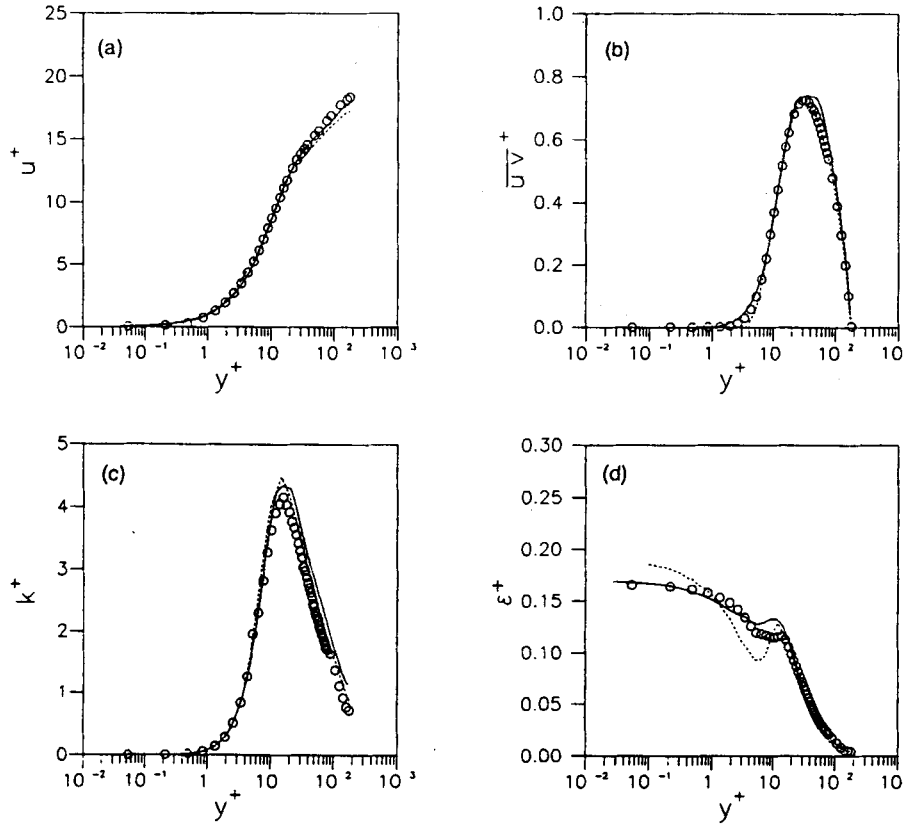

Figure 2. Profiles of (a) U^+, (b) $-\overline{uv}^+$, (c) k^+ and (d) ε^+ for 2D channel flow, $Re_\tau = 180$: ○, DNS; – – –, RMM; ———, present model

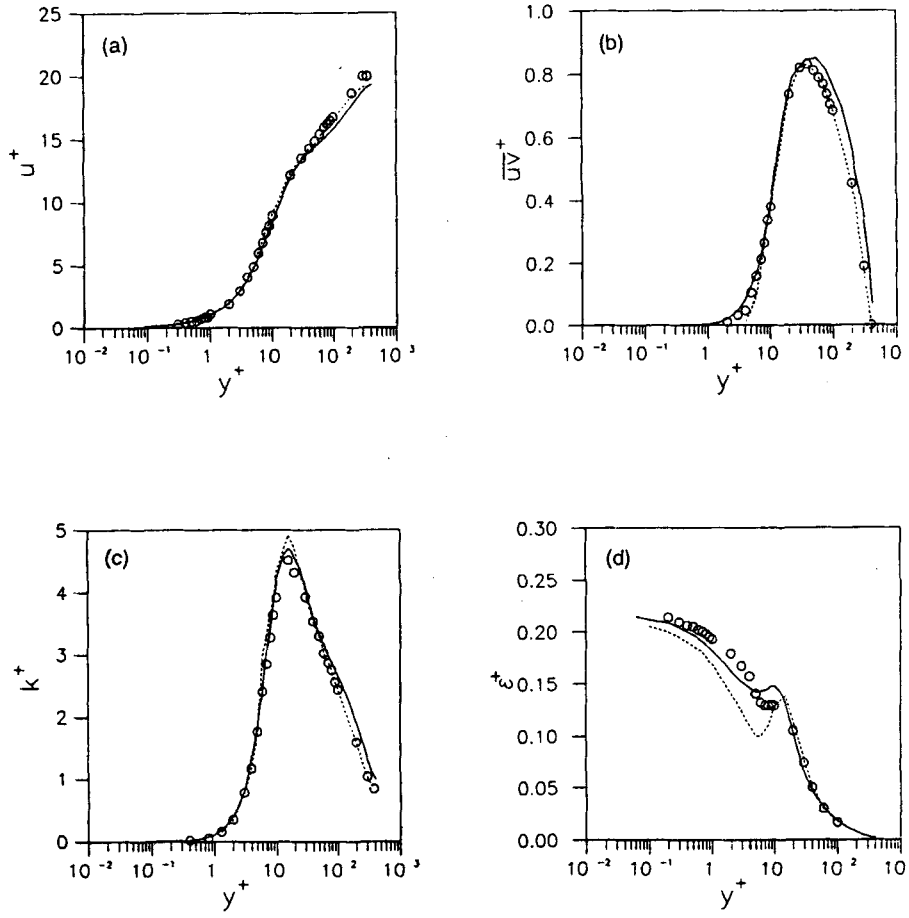

Figure 3. Profiles of (a) U^+, (b) $-\overline{uv}^+$, (c) k^+ and (d) ε^+ for 2D channel flow, $Re_\tau = 395$: ○, DNS; — — —, RMM; ——, present model

The two models predict similar slopes for the shear stress around $y^+ = 5$, both being slightly above the DNS data. The k^+ profiles depicted in Figures 2(c)–4(c) illustrate the correct growth rate of k achieved by both models, while the peak is better calculated by the PR model. However, the DNS dissipation profile is evidently reproduced much better with the present model (Figures 2(d) and 3(d)). This implies that the growth rate of k should also be more correct, since near the wall $k^+ = a_k y^+$ and $\varepsilon_w^+ = 2a_k$. It is encouraging to observe that both the variation across the channel and the Reynolds number dependence of the k and ε profiles have been adequately captured by the proposed model. The impact of the new term is clearly evident and the over/underestimation of ε^+ in the near-wall region ($y^+ = 0$–20) produced by most low-Re models has now been significantly reduced.

Figures 5(a)–5(d) compare predictions of the present model for a ZPG boundary layer at $Re_\theta = 1410$ with the DNS data of Spalart.[18] All four turbulent quantities have been reproduced quite accurately, suggesting the ability of the model to faithfully capture the Reynolds number variation of the near-wall turbulent parameters under investigation. Referring back to Figure 1(c), the ε_w^+ variation with Re_θ is reproduced well, while the skin friction shown in Figure 6, where data of References 30 and 31 up to $Re_\theta = 16,465$ are displayed, is predicted to within 4·5%.

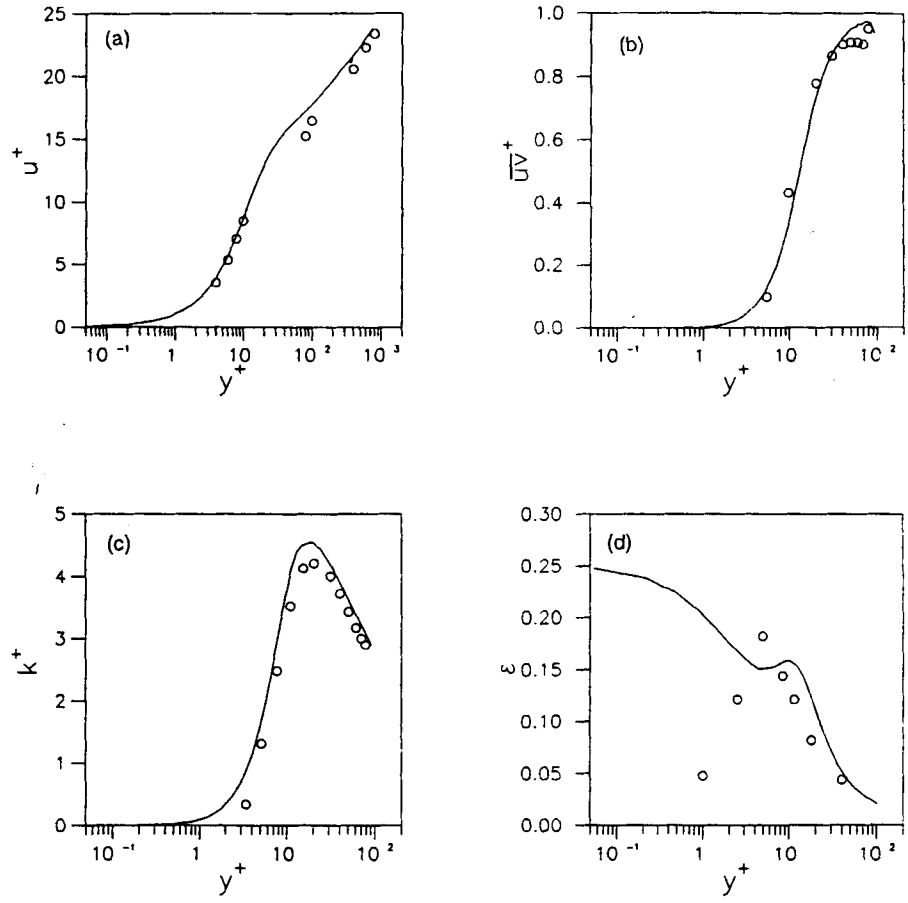

Figure 4. Profiles of (a) U^+, (b) $-\overline{uv}^+$, (c) k^+ and (d) ε^+ for 2D channel flow, $Re_\tau = 1052$: ○, experiment;[29] ——, present model

4.2. Boundary layers developing in adverse or favourable pressure gradients and under geometry-induced separation

The data of Nagano *et al.*[32] were chosen for comparison with predictions, since they reported detailed turbulence measurements. The boundary layer studied develops under a strong adverse pressure gradient nearly approaching separation ($H = 1{\cdot}9$). The described calculations were obtained by utilizing the model correction on $c_{\varepsilon 1}$ discussed previously. This is not dependent on the flow configuration and has been correlated to the physics of the wall region. More importantly, the same form of the model has been applied to all three flow cases (ZPG, APG, FPG). Figures 7(a)–7(d) illustrate the four calculated turbulent quantities at axial stations half-way ($x = 0{\cdot}523$) along and near the top end ($x = 0{\cdot}925$) of the linearly varying pressure gradient. All three measured quantities ($U, \bar{uv}, k$) have been calculated well at all four measured stations, while the dissipation, which was not measured, is simply included here to display the impact of the new term used in the ε equation. Skin friction coefficients have also been predicted well for the four measured stations as shown in Figure 8. Satisfactory predictions for this flow have also been reported by Hattori *et al.*,[35] but their k–ε model was used in conjunction with an algebraic stress model.

Subsequently, the relaminarizing boundary layer of Patel and Head[33] developing in a strong favourable pressure gradient was calculated. The prediciton of the skin friction, shown in Figure 9

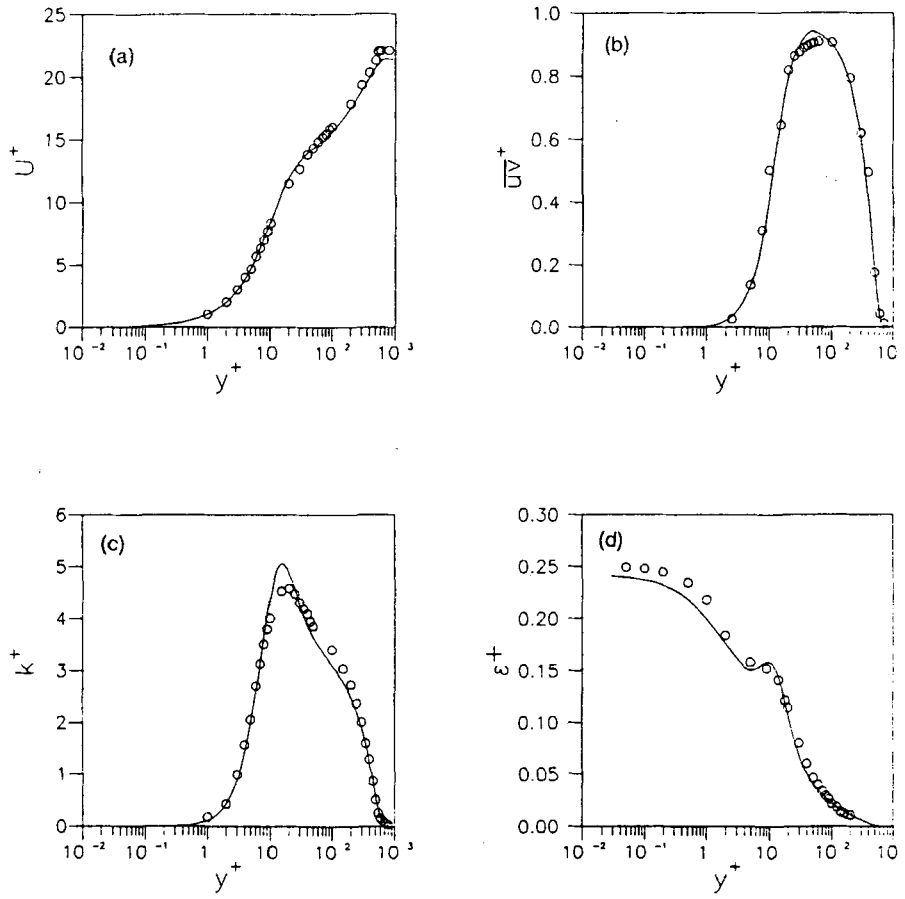

Figure 5. Profiles of (a) U^+, (b) $-\overline{uv}^+$, (c) k^+ and (d) ε^+ for 2D boundary layer flow, $Re_\theta = 1410$: ○, DNS; ——, present model

compared with measurements, clearly suggests that the model reproduces accurately the succession of stages occurring in this type of flow: the initial increase in skin friction under the steep acceleration ($P^+ = (\nu/\rho u_\tau^3)\mathrm{d}P/\mathrm{d}x$ up to -3×10^{-2}) is followed by a rapid decay due to relaminarization.

The rearward-facing step of Driver and Seegmiller[34] was next calculated to perform an initial test of the model's ability to cope with separated flows. Zero-top-wall-angle flow with an inlet Re of 3×10^5 was chosen for the calculation. The calculational domain extended from four step heights upstream to 32 step heights downstream of the step and was covered by a 90×120 (y,x) mesh clustered near the wall and in the recirculation zone. Figure 10 shows the predicted and measured distributions of the skin friction coefficient c_f along the bottom wall. A c_f comparison is considered an illustrative and stringent test for separated flows.[3,4] The plot suggests a moderate overprediction of the negative c_f with an adequate reproduction of the redeveloping skin friction data. The reattachment length is slightly overpredicted (by 10%). Overall the model's performance is seemed satisfactory, but it should be noticed that details in near-wall modelling may be less important in this case, since flow development is determined by the modelling of the free shear layer detaching at the step corner.

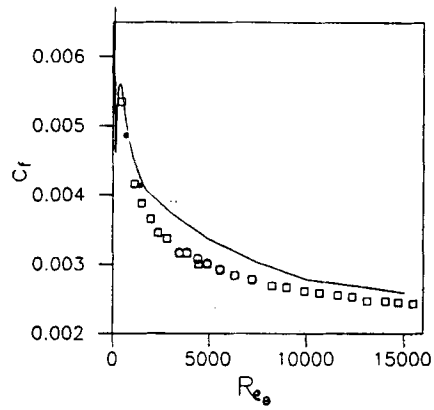

Figure 6. Skin friction distribution for turbulent flat plate boundary layer: □, ○, experiment;[30,31] ●; ——, present model

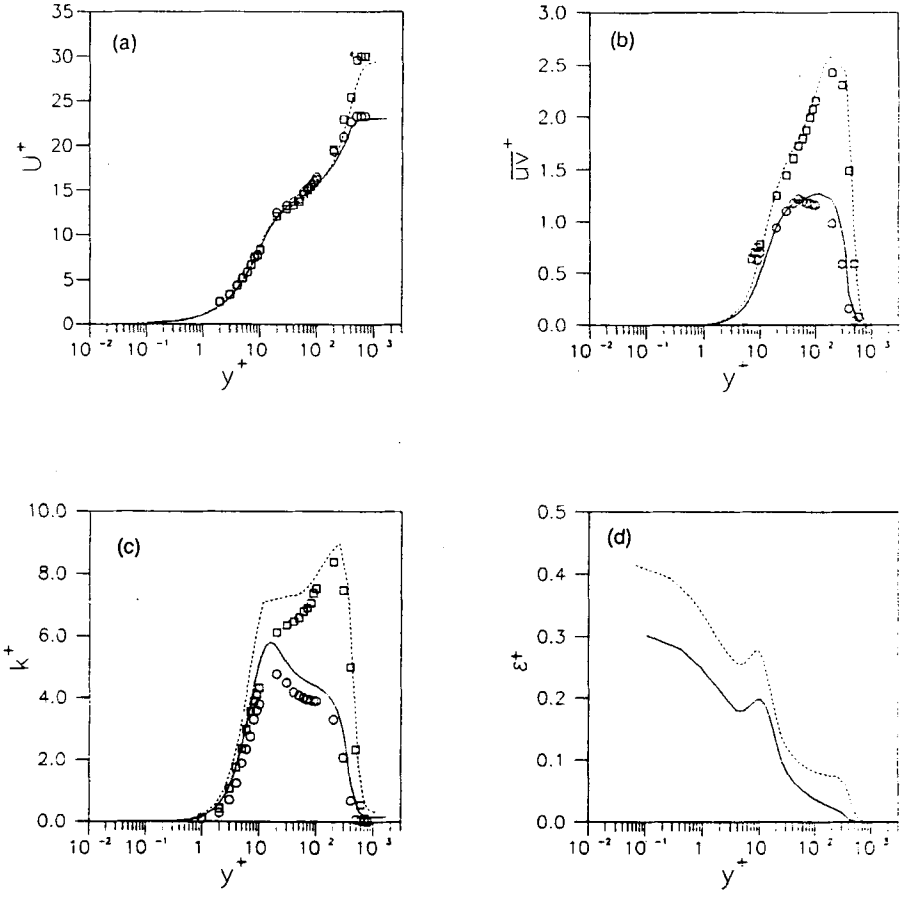

Figure 7. Profiles of (a) U^+, (b) $-\overline{uv}^+$, (c) k^+ and (d) ε^+ for 2D boundary layer flow in adverse pressure gradient (Nagano *et al.*[32] flow): ○, experiment, $x = 0{\cdot}523$; □, experiment, $x = 0{\cdot}925$; ——, – – –, present model

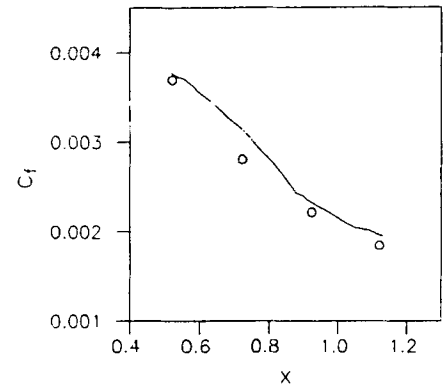

Figure 8. Skin friction prediction for Nagano *et al.*[32] flow: ○, experiment; ———, present model

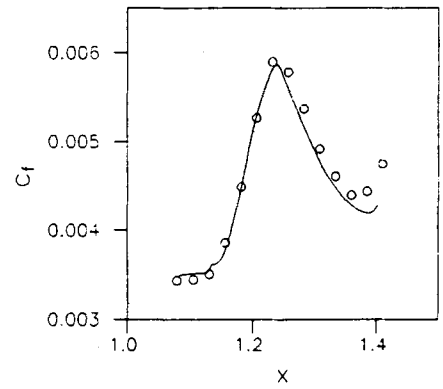

Figure 9. Skin friction prediction for 2D boundary layer in favourable pressure gradient (Patel and Head[33] flow): ○, experiment; ———, present model

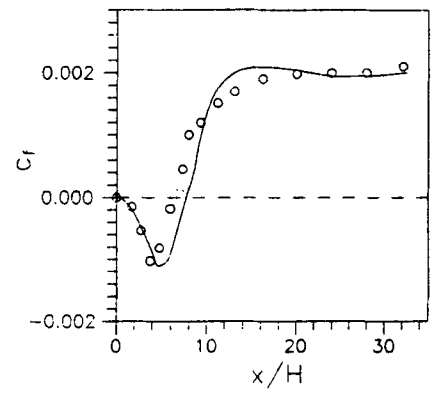

Figure 10. Skin friction distribution for flow over a backward-facing step

5. CONCLUDING REMARKS

A low-Reynolds-number k–ε model has been formulated and predictions were successfully compared with DNS and experimental data for a range of complex shear layers. Novel features of the model include the implementation of a new form of damping function to account for both 'wall proximity' effects and viscosity influences and the introduction of a more flexible damping argument in the light of experimental results. Additionally, a new term introduced into the ε has substantially improved the prediction of the near-wall dissipation profile. A self-consistent, non-flow-specific model modification enabled the successful use of the same model form for the range of zero, adverse and favourable pressure gradient boundary layers as well as backward-facing-step separated flows calculated.

Before the general usefulness of the model is established, much wider testing is needed, perhaps particularly in separating and recirculating flows where flow separation is not induced by a geometric discontinuity.

ACKNOWLEDGEMENT

N.C.K. gratefully acknowledges the financial support of the Greek Industry Association.

REFERENCES

1. B. E. Launder and D. B. Spalding, 'The numerical computation of turbulent flow', *Comput. Methods Appl. Mech. Eng.*, **3**, 269–289 (1974).
2. W. Rodi, *Turbulence Models and Their Application in Hydraulics*, International Association for Hydraulic Research, Delft, 1980.
3. B. E. Launder, 'Numerical computation of convective heat transfer in complex turbulent flows: time to abandon wall functions?', *Int. J. Heat Mass Transfer*, **27**, 1485–1491 (1974).
4. W. Rodi, 'Some current approaches in turbulence modelling', *AGARD AR-329*, 1989.
5. W. P. Jones and B. E. Launder 'The calculation of low Reynolds-number phenomena with a two equation model of turbulence', *Int. J. Heat Mass Transfer*, **16**, 1119–1130 (1973).
6. D. R. Chapman and G. D. Kuhn, 'The limiting behaviour of turbulence near the wall', *J. Fluid Mech.*, **170**, 265–292 (1986).
7. T. H. Shih and J. L. Lumley, 'Kolmogorov behaviour of near wall turbulence and its applications in turbulence modelling', *J. Comput. Fluid Dyn.*, **1**, 43–56 (1993).
8. V. C. Patel, W. Rodi and G. Scheurer, 'Turbulence models for near wall and low Reynolds number flows: a review', *AIAA J.*, **23**, 1308–1319 (1985).
9. N. J. Lang and T. H. Shih, 'A critical comparison of two equation turbulence models', *ICOMP Report 91–15*, 1991.
10. V. Michelassi and T. H. Shih, 'Low-Reynolds number two-equation modelling of turbulent flows, *ICOMP Report 91–06*, 1991.
11. V. Michelassi 'Adverse pressure gradient flow computation by two equation turbulence models', in W. Rodi and F. Martelli (eds), *Engineering Turbulence Modelling and Experiments*, Vol. 2, Elsevier, Amsterdam, 1993.
12. P. R. Spalart, 'Numerical study of sink flow boundary layers', *J. Fluid Mech.*, **172**, 307–328 (1986).
13. V. Yakhot and S. A. Orszag, 'Renormalization group analysis of turbulence I. Basic theory', *J. Sci. Comput.*, **1**, 3–51 (1986).
14. Y. Zhou and C. G. Speziale, 'An overview of RNG methods in turbulence modelling: panel discussion summary', *ICASE/ LaRC Workshop on Transition, Turbulence and Combustion*, June 1993.
15. V. Yakhot, S. A. Orszag, S. Thangam, T. B. Gatski and C. G. Speziale, 'Development of turbulence models for shear flows by double expansion technique', *Phys. Fluids A*, **4**, 151–167 (1992).
16. N. N. Mansour, J. Kim and P. Moin, 'Reynolds-stress and dissipation-rate budgets in a turbulent channel flow', *J. Fluid Mech.*, **124**, 14–44 (1988).
17. J. Kim, unpublished DNS data, 1990.
18. P. R. Spalart, 'Direct simulation of a turbulent boundary layer up to $Re_\theta = 1410$', *J. Fluid Mech.*, **187**, 61–98 (1988).
19. R. Kessler, 'Near wall modelling of the dissipation rate equation with DNS data', in W. Rodi and F. Martelli (eds), *Engineering Turbulence Modelling and Experiments*, Vol. 2, Elsevier, Amsterdam, 1993, pp. 113–122.
20. V. Michelassi, W. Rodi and G. Scheurer, 'Testing a low Reynolds number k–ε turbulence model based on DNS data', *Proc. 8th Symp. on Turbulent Shear Flows*, Munich, September 1991.
21. Z. Yang and T. H. Shih, 'A k–ε model for turbulent and transitional boundary layers', in R. M. C. So, C. G. Speziale and B. E. Launder (eds), in *Near Wall Turbulent Flows*, Elsevier, Amsterdam, 1993.
22. M. J. Lee, J. Kim and P. Moin, 'Structure of turbulence at high shear rate', *J. Fluid Mech.*, **216**, 561–583 (1990).
23. W. J. Devenport and E. P. Sutton, 'Near wall behaviour of separated and reattaching flows', *AIAA J.*, **29**, 25–31 (1991).

24. K. Hanjalic and S. Jakirlic, 'A model of stress dissipation in second moment closures', in F. Niewstadt *et al.* (eds), *Proc. 4th Eur. Turbulence Conf.*, Delft, Kluwer Dordrecht, 1992.
25. E. W. Miner, T. F. Swean, R. A. Handler and R. Leighton, 'Examination of wall damping for the k–ε model using direct simulations of turbulent channel flow', *Int. j. numer. methods fluids*, **12**, 609–624 (1991).
26. W. Rodi and G. Scheurer, 'Scrutinizing the k–ε turbulence model under adverse pressure gradient conditions', *J. Fluids Eng.*, **108**, 174–179 (1986).
27. S. V. Patankar, *Numerical Heat Transfer and Fluid Flow*, McGraw-Hill, New York, 1980.
28. P. Koutmos, 'An isothermal study of gas turbine combustor flows', *Ph.D. Thesis*, University of London, 1985.
29. J. Laufer, 'The structure of turbulence in fully developed pipe flow', *NACA Report 1174*, 1954.
30. K. Wieghardt and W. Tillmann, 'On the turbulent friction layer for rising pressure', *NACA TM 1314*, 1951.
31. P. S. Klebannoff, 'Characteristics of turbulence in a boundary layer with zero pressure gradient', *NACA Rep 1247* 1955.
32. Y. Nagano, M. Tagawa and T. Tsuji, 'Effects of adverse pressure gradients on mean flows and turbulence statistics in a boundary layer', in *Turbulent Shear Flows*, Vol. 8, Springer, Berlin, 1992.
33. V. C. Patel and M. R. Head, 'Reversion of turbulent to laminar flow', *J. Fluid Mech.*, **34**, 371–392 (1968).
34. D. H. Driver and H. L. Seegmiller, 'Features of a reattaching turbulent shear layer in divergent channel flow', *AIAA J.*, **23**, 163–171 (1985).
35. H. Hattori, Y. Nagano and M. Tagawa, 'Analysis of turbulent heat transfer under various thermal conditions with two-equation models', in W. Rodi and F. Martelli (eds), *Engineering Turbulence Modelling and Experiments*, Vol. 2, Elsevier, Amsterdam, 1993.